PERGAMON

PII: S1359-6454(99)00036-1

Acta mater. Vol. 47, No. 5, pp. 1417–1424, 1999

Printed in Great Britain
1359-6454/99 $20.00 + 0.00

THEORETICAL INVESTIGATION OF SULFUR SOLUBILITY IN PURE COPPER AND DILUTE COPPER-BASED ALLOYS

P. A. KORZHAVYI†, I. A. ABRIKOSOV and B. JOHANSSON

Condensed Matter Theory Group, Physics Department, Uppsala University, S-75121 Uppsala, Sweden

(Received 19 June 1998; accepted 12 January 1999)

Abstract—Dilute Cu-based alloys containing S, P, and Ag impurities and also vacancies are studied theoretically on the basis of total energy calculations. This is done within the supercell approach by using the locally self-consistent Green's function (LSGF) method. The impurity solution energies, volume misfits, and interaction energies for these defects are calculated and used to study the microscopic mechanism behind the effect of these impurities on embrittlement of copper at intermediate temperatures. It is shown that the solubility of S in Cu is low due to precipitation of the highly stable Cu_2S phase. A large binding energy of a sulfur–vacancy defect pair in the first coordination shell (–0.46 eV) and a sulfur–sulfur defect pair in the second coordination shell (–0.12 eV) seem to favor this precipitation. The effect of phosphorus and silver impurities on the bulk S solubility has also been studied, and was found to depend on the competition of these impurities with sulfur for vacancies, as well as probably for other lattice defects.

1. INTRODUCTION

Application of pure, oxygen-free copper as a construction material having excellent corrosion resistance is limited because of the effect of intergranular embrittlement at temperatures above 100–150°C. Intergranular cavitation and fracture were observed preferentially at random grain boundaries [1] and the fracture surface was found to be enriched in sulfur [2]. Thus, there is strong evidence that this embrittlement is caused by grain boundary segregation of sulfur. The sulfur content in commercially pure copper is very low, but it is nevertheless well above the equilibrium solubility of sulfur in copper. A drop in ductility was observed even for ultra-high purity copper [3].

At the same time, it is of considerable interest that a certain amount of phosphorus or silver additions to copper has been found to improve its ductility at intermediate temperatures (180–450°C) [2]. However, the microscopic mechanism of this phenomenon is not clear. Two possible explanations have been proposed: the ductility improvement could be either due to an increase in the S solid solubility or due to a segregation of P or Ag and a competition with S for the grain boundary sites [2]. Thus, reliable information on the interactions of these impurities with each other and with other defects in Cu is highly desirable.

It is not known what structure the segregated sulfur forms at grain boundaries. Judging from the equilibrium Cu–S phase diagram [4], it is natural to expect formation of copper(I) sulfide (Cu_2S). It is noteworthy that stoichiometric Cu_2S may exist in three crystal structures: low chalcocite (αCh, monoclinic), high chalcocite (βCh, hexagonal), and high digenite (Dg, cubic). The temperatures of the structural transformations in Cu_2S, 103.5°C (αCh $\rightleftarrows$ βCh) and 435°C (βCh $\rightleftarrows$ Dg), correlate with the embrittlement temperatures of copper. Therefore, the structural properties of copper sulfide as well as the thermodynamics and kinetics of the solid state reactions in the Cu–S system are important for understanding the mechanism of medium temperature embrittlement of copper.

The solubility of sulfur in copper was determined experimentally [5, 6] at high temperatures in the range from 600 to 1000°C. In this temperature interval the solid solution of S in Cu is in equilibrium with the high digenite phase. High digenite has the antifluorite cF12 structure with sulfur atoms arranged in a face-centered cubic (f.c.c.) lattice and copper atoms occupying all the tetrahedral interstitial sites. Alternatively, this structure may be viewed as a simple cubic lattice of copper atoms with the centers of the cubes half-occupied by sulfur atoms in staggered order as shown in Fig. 1(a). It is also known from experiment [7–9] that additional copper vacancies easily form in the off-stoichiometric digenite $Cu_{2-x}S$.

Due to the large vacancy content the coordination number of Cu atoms in Cu_2S is reduced compared to that in f.c.c. Cu. Because of the low coordination number the diffusion of Cu in copper sulfides is very fast [10]. The diffusion of sulfur in copper is also anomalous [11]. Among all the substitutional impurities in Cu considered in Ref. [11], S has the largest diffusion coefficient in the bulk

†To whom all correspondence should be addressed.

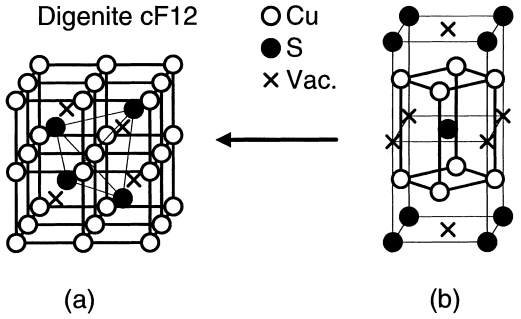

Fig. 1. (a) Crystal structure of the high-temperature Cu_2S phase (high digenite). (b) A low-energy concentrated defect configuration favored by the sulfur–sulfur, sulfur–vacancy, and vacancy–vacancy interactions in the f.c.c. copper.

and a high diffusivity at grain boundaries. At the same time, sulfur was found to reduce the self-diffusivity of Cu at grain boundaries [12]. One possible way of explaining the diffusion anomalies in f.c.c. Cu is to consider so-called correlation effects which originate from strong impurity–vacancy interactions. In this connection, the presence of vacancies and their interaction with other impurities in Cu (like S, P, and Ag, considered in the present study) is also of importance. There is no experimental information available about the interactions of S, P, and Ag impurities with each other or with vacancies, although such kind of data can be found for some other impurities in copper [13].

Theoretically, the electronic structure and physical properties of S, P, and Ag impurities in Cu have been calculated by several authors [14–17]. It has been shown that sulfur and phosphorus form bound 3s states below the bottom of the copper valence band, while Ag forms a virtual bound 4d state below the bottom of the copper d-band. Solution energies of 3d impurities in Cu have been calculated by Drittler *et al.* using the Korringa–Kohn–Rostoker (KKR) method within the Green's function formalism [18]. First-principles calculations also exist for 3d and 4sp impurities as well as for 4d and 5sp impurities in Cu. Interactions between selected defects in Cu [19–22] and an effect of local lattice relaxations around the defects [23, 24] have recently been considered. However, to our knowledge no total energy calculations for S or P impurities in Cu have been performed so far.

The electronic structure with respect to structural and cohesive properties of more than 30 transition metal sulfides have been investigated by Raybaud *et al.* using the Vienna *ab initio* simulation program (VASP) with the aim of establishing a correlation between the strength of the metal–sulfur bond and the catalytic activities of these materials [25, 26]. Unfortunately, the noble metal sulfides were not part of this systematic study. Structural properties of copper and silver sulfides have been investigated in the framework of a semiempirical tight-binding approach [27]. It was shown that in noble metal(I) sulfides the local three- and four-fold anion configurations are very close in energy. This is the basic reason for why copper sulfides show a variety of local anion configurations depending on the chemical composition and temperature.

In the present work we perform a first-principles theoretical investigation of point defects and their interactions in dilute copper-based alloys. The phase equilibrium between the f.c.c. solid solution of S in Cu and the Cu_2S high digenite phase is studied. The role of defect interactions in the thermodynamics and kinetics of supersaturated Cu–S solid solution decomposition is discussed.

2. METHOD OF CALCULATIONS

2.1. Thermodynamic relations

The concentration $c_0(T)$ of the terminal solid solution of an element X (X = S, P, Ag or some other element) in Cu at a temperature T can be found from an analysis of the following dissolution reaction [28] describing the equilibrium between the solid solution (ss) and the adjacent intermediate phase of the stoichiometric composition Cu_kX_m:

$$Cu_kX_m \rightleftarrows k\mathrm{Cu(ss)} + m\mathrm{X(ss)}. \qquad (1)$$

The energy of this reaction is a key thermodynamic quantity which determines the equilibrium solubility. All the solute elements considered in this work form dilute substitutional alloys with copper. Therefore, with a sufficient accuracy they may be treated as ideal solid solutions and within the mean-field approximation for the configurational entropy. Upon these assumptions the solvus line may be expressed as

$$c_0(T) \simeq \exp[-Q_X/k_BT] \qquad (2)$$

where Q_X is the energy of the dissolution reaction, equation (1), per one solute atom X(ss), and k_B is Boltzmann's constant.

In cases where the adjacent phase is a pure component X, the energy of the dissolution reaction becomes equivalent to the impurity solution energy which is defined relative to pure alloy components. Theoretically, the impurity solution energy may be calculated [18] as a derivative of the alloy mixing energy $E^{\mathrm{mix}}_{\mathrm{Cu-X}}$ with respect to concentration c of the solute

$$E^{\mathrm{imp}}_{\mathrm{X}} = \left.\frac{\mathrm{d}E^{\mathrm{mix}}_{\mathrm{Cu-X}}(c)}{\mathrm{d}c}\right|_{c=0} \qquad (3)$$

where $E^{\mathrm{mix}}_{\mathrm{Cu-X}}(c)$ is, in turn, calculated from the total energies E^{tot} of $Cu_{1-c}X_c$ random alloys and pure alloy components taken at their respective equilibrium volumes

$$E^{\mathrm{mix}}_{\mathrm{Cu-X}}(c) = E^{\mathrm{tot}}_{\mathrm{Cu}_{1-c}\mathrm{X}_c} - (1-c)E^{\mathrm{tot}}_{\mathrm{Cu}} - cE^{\mathrm{tot}}_{\mathrm{X}}. \qquad (4)$$

The relation between the energy of dissolution reaction and the impurity solution energy is given by

$$Q_{\mathrm{X}} = E^{\mathrm{imp}}_{\mathrm{X}} - \frac{k+m}{m} E^{\mathrm{f}}_{\mathrm{Cu}_k\mathrm{X}_m} \tag{5}$$

where $E^{\mathrm{f}}_{\mathrm{Cu}_k\mathrm{X}_m}$ is the formation energy of the $\mathrm{Cu}_k\mathrm{X}_m$ compound (per atom):

$$E^{\mathrm{f}}_{\mathrm{Cu}_k\mathrm{X}_m} = \frac{1}{k+m} E^{\mathrm{tot}}_{\mathrm{Cu}_k\mathrm{X}_m} - \frac{k}{k+m} E^{\mathrm{tot}}_{\mathrm{Cu}} - \frac{m}{k+m} E^{\mathrm{tot}}_{\mathrm{X}}. \tag{6}$$

Note, that the impurity solution energy as well as the formation energy of an intermediate compound depend on the standard state of the solute. In this work the standard states of the pure components are chosen to be f.c.c. Cu and Ag in agreement with experiment, whereas S and P are treated in the b.c.c. crystal structure which is not the observed equilibrium structure. The vacancy formation energy can also be calculated from equations (3) and (4) by taking the energy of the standard state for vacancies $E^{\mathrm{tot}}_{\mathrm{Vac}} \equiv 0$. The fact that for S and P we use non-equilibrium standard states should be taken into account when analyzing the calculated solution and formation energies. At the same time, Q_{X} does not depend on $E^{\mathrm{tot}}_{\mathrm{X}}$, i.e. one may consider any appropriate crystal structure for pure X, not only its equilibrium crystal structure. This eliminates the necessity of dealing with a complicated equilibrium crystal structure of S thus considerably reducing the amount of computational work. The graphic representation of equation (5) is given in Fig. 2.

Another important thermodynamic characteristic of a dilute alloy is the concentration dependence of the atomic volume in solid solutions that is commonly referred to as the volume misfit. For a cubic crystal lattice the volume misfit is related to the variation of the lattice parameter, a, with concentration as

$$\delta \equiv \frac{1}{\Omega}\frac{\mathrm{d}\Omega}{\mathrm{d}c}\bigg|_{c=0} = \frac{3}{a}\frac{\mathrm{d}a}{\mathrm{d}c}\bigg|_{c=0} \tag{7}$$

where Ω is the equilibrium volume per atom.

Finally, an interaction energy $E^{\mathrm{int}}_{\mathrm{X-Y},n}$ between two defects X and Y separated by a distance of the nth coordination shell radius is defined as a difference in total energy of a system which contains this defect pair, $E^{\mathrm{tot}}_{\mathrm{X-Y},n}$, and of a system where these defects are isolated, $E^{\mathrm{tot}}_{\mathrm{X-Y},\infty}$

$$E^{\mathrm{int}}_{\mathrm{X-Y},n} = E^{\mathrm{tot}}_{\mathrm{X-Y},n} - E^{\mathrm{tot}}_{\mathrm{X-Y},\infty}. \tag{8}$$

By definition, a negative sign of the interaction energy corresponds to an attraction between the defects.

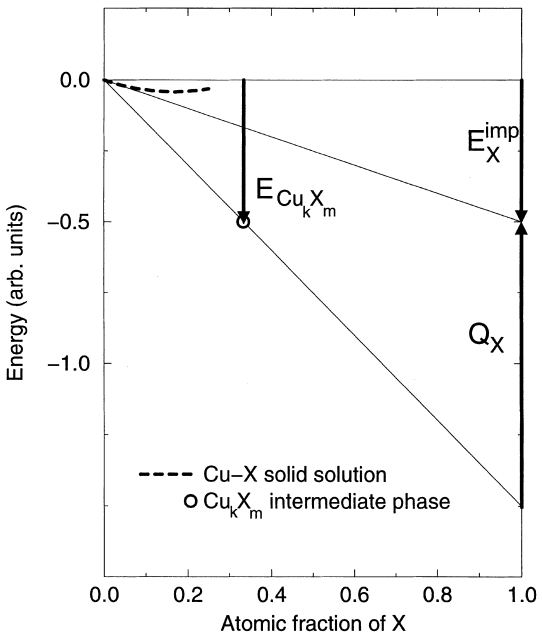

Fig. 2. Schematic representation of the phase equilibrium between Cu–X solid solution and a stoichiometric $\mathrm{Cu}_k\mathrm{X}_m$ intermediate phase. Mixing energy of the solid solution as a function of the solute concentration is shown by a dashed line. The formation energy of the $\mathrm{Cu}_k\mathrm{X}_m$ phase ($E^{\mathrm{f}}_{\mathrm{Cu}_k\mathrm{X}_m}$), the impurity solution energy ($E^{\mathrm{imp}}_{\mathrm{X}}$), and the energy of the dissolution reaction (Q_{X}) are indicated by arrows. The lengths and the directions of the arrows represent the absolute values and the signs, respectively, of the corresponding quantities.

2.2. *Computation details*

In this work we model the dilute copper-based alloys by large supercells containing up to as many as 108 lattice sites. In doing so we take advantage of a new generation of electronic structure methods in which the computer time scales linearly with number of atoms N [29–32]. In particular, we employ the locally self-consistent Green's function (LSGF) method by Abrikosov *et al.* [31, 32], which is one of the most efficient so-called order-N methods, and which has been successfully applied to a number of ordered, disordered, and partially ordered metallic systems.

The LSGF method is based on the linear muffin-tin orbitals (LMTO) theory of Andersen [33–38]. We employ the atomic sphere approximation (ASA) for the one-electron potential corrected by including higher multipoles of the electron density in the expansion of the electrostatic potential and energy. This so-called ASA + M technique allows one to obtain surface energies [39] and vacancy formation energies [40] for transition and noble metals with an accuracy typical for the most precise full-potential (FP) methods.

To study monovacancies and single impurities of S, P, and Ag in Cu we use $2 \times 2 \times 2$ (32 sites) and $3 \times 3 \times 3$ (108 sites) f.c.c. Cu-based supercells con-

taining one point defect per supercell. The difference between the impurity solution energies calculated using 32- and 108-site supercells was found to be about 0.01 eV for the S and P impurities as well as for vacancies in Cu. For the Ag impurities a somewhat larger difference of about 0.05 eV was found. This shows that the defects may be regarded as nearly isolated even in a 32-site supercell where they are separated by a distance of 8th coordination shell from each other.

Impurity–impurity and vacancy–impurity pair interactions are calculated using $2 \times 2 \times 4$ (64 sites) supercells containing two point defects in different pair combinations and spatial configurations as shown in Fig. 3. The two defects of each defect pair were first considered at the largest possible separation distance between them (8th coordination shell) and then they were drawn together to become first or second nearest neighbors. The corresponding total energy change gives an estimate of the defect interaction energy, equation (8).

We have performed scalar-relativistic total energy calculations of the dilute Cu-based alloys and ordered copper sulfide Cu_2S (high digenite). To make the structure of Cu_2S appear more close-packed in the theoretical treatment, we introduced empty spheres into the octahedral interstitial positions of the f.c.c. sulfur sublattice. The vacancies in the f.c.c. Cu have also been modeled by empty spheres. We used equal atomic sphere radii for all atoms as well as for the empty spheres in order to have a consistent description of various defect configurations in the dilute and concentrated alloys considered in this work. Changing the atomic sphere radii ratio $R_{S,Vac}/R_{Cu}$ from 1 to 1.08 (the latter value may be obtained from the matching of the potentials at the sphere boundaries of S and Cu) changes the total energy of the Cu_2S compound by 0.03 eV/atom. This value, as will be shown below, is much less than the typical energies involved.

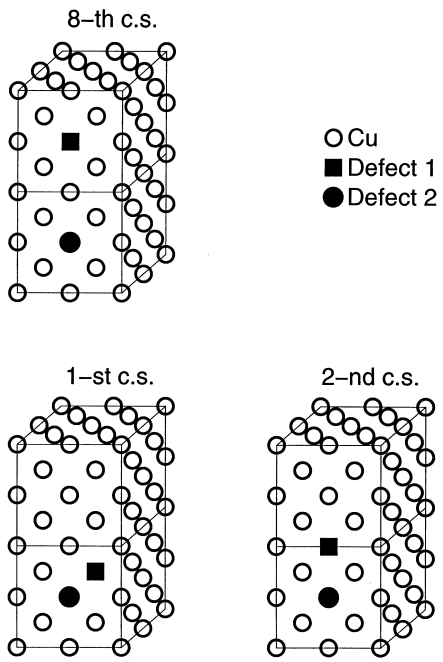

Fig. 3. Constitution of the $2 \times 2 \times 4$ f.c.c. supercells with 64 lattice sites which were used in the present work to calculate defect interactions.

In the present study we used the angular momentum cutoff $l_{max} = 2$ for the Green's function as well as for the wave function expansion. Correspondingly, non-spherical components of the charge density inside the atomic spheres up to $l = 4$ were taken into account. Thus, we treated valence s, p, and d electrons self-consistently within the local density approximation (LDA) for which we used the Perdew and Zunger parametrization [41] of the many-body results by Ceperley and Alder [42]. The core states were recalculated at each self-consistency loop using the soft core approximation. The Brillouin zone integration was performed by means of the special point technique, including 240 **k**-points in the 1/48 irreducible wedge of the Brillouin zone for the f.c.c. lattice.

The moments of the state density were evaluated by a 20 point gaussian integration on a complex energy contour enclosing the occupied states. Since 3p impurities like S and P form 3s bound states below the bottom of the valence band of Cu [16, 17], we had to choose a very large contour diameter of 1.5 Rydberg for the complex energy integration. Therefore, we did not use the LMTO parametrization of the potential function in terms of so-called potential parameters, but calculated its exact values at each energy point of the contour.

For each supercell we performed self-consistent calculations of the electronic structure and the total energy at four different lattice parameters close to the equilibrium. The equilibrium atomic volumes and total energies at equilibrium were calculated using a third order polynomial fit to the results of the self-consistent calculations. Thus, global relaxation of the crystal volume was taken into account in our calculations whereas the effect of local lattice relaxations was neglected.

3. RESULTS

3.1. Single impurities in Cu: solution energies and volume misfits

The calculated impurity solution energies and the energies of the dissolution reaction for S, P, and Ag impurities as well as for vacancies in Cu are presented in Table 1, where we also show the available corresponding experimental data. The calculated and experimental volume misfits are compared in Table 2. The experimental value of the energy of the dissolution reaction $Q_S \approx 1.0$ eV was deduced from the measured solubility [5, 6] with the help of

Table 1. Impurity solution energy, E_X^{imp}, and energy of the dissolution reaction, Q_X, for selected point defects in Cu, see text. All values are given in eV/atom

Defect, X	E_X^{imp}	Q_X		
		This work	FP calculation	Experiment
S	0.02	1.21		1.0 ± 0.1[b]
P	−0.29	—		
Ag	0.83	0.83		0.39[c]
Vac	1.44	1.44	1.41[a]	1.28 ± 0.05[d]

[a]Full-potential calculation, Ref. [43].[b]Estimated from experimental solubility, Refs [5, 6].[c]Experiment, Ref. [44].[d]Experiment, Ref. [13].

equation (2). It compares well with the calculated energy of the dissolution reaction of sulfur in copper, and indicates that the theoretical estimate of solubility of S in the bulk f.c.c. Cu is very low indeed. The solubility is low not due to the fact that sulfur impurity does not "fit" into a substitutional position in the f.c.c. Cu matrix (the volume misfit is found to be less than 45%), but because of a high stability of copper(I) sulfide (Cu_2S). Its energy of formation is calculated to be −0.39 eV/atom which correlates reasonably well with the experimental standard enthalpy of formation of high digenite [46] extrapolated to zero temperature, −0.34 eV/atom (because of the difference in the standard states a direct comparison of the calculated and experimental formation energies is not possible).

Silver atoms do not form ordered phases with copper, and as silver and copper belong to the same subgroup in the Periodic Table, the chemical contribution to the impurity solution energy is relatively small. In this case, the atomic size mismatch gives the main contribution. Our calculations give qualitatively the correct solution energy and volume misfit of Ag impurity in Cu, but the numerical values seem to be too high when compared with experiment. This discrepancy is mainly caused by the high relaxation energy around a silver impurity in copper. This energy is about 0.25 eV according to full-potential calculations of Papanikolaou *et al.* [24]. The energy of local relaxation around the other impurities in Cu considered in this work is expected to be smaller. For instance, it is only 0.07 eV for a vacancy in Cu [24]. Accordingly, the vacancy formation energy in Cu (see Table 1) and the value of the volume misfit (see Table 2) calculated in this work, are in good agreement with experiment as well as with the results of more accurate full-potential calculations. For a phosphorus impurity in copper our calculations give a small value of the volume misfit, which agrees well with experiment.

Table 2. Calculated and experimental volume misfits for selected point defects in Cu

Defect	This work	FP calculation	Experiment
S	+0.32		
P	+0.11		+0.10[b]
Ag	+0.64	+0.52[a]	+0.45[b], +0.58[b]
Vac	−0.25	−0.3[a]	−0.25[c]

[a]Full-potential calculation, Ref. [24].[b]Experiment, Ref. [45], from $a(c)$ data.[c]Experiment, Ref. [13].

3.2. *Defect interaction energies in Cu-based alloys*

The calculated defect interaction energies are listed in Table 3. As expected, we find a strong attraction between S impurity and a vacancy in Cu when they are nearest neighbors. This interaction is partially due to a reduction of strain energy in the S–Vac pair (the volume misfits of sulfur and vacancy have opposite signs, as can be seen from Table 2). The other origin of the sulfur–vacancy attraction is the reduction of the local coordination number of the sulfur atom in the S–Vac pair, which becomes closer to the local coordination number of sulfur in copper sulfide Cu_2S. As a consequence, the S impurity must have an affinity to crystal defects (vacancies, dislocations, grain boundaries, or open surfaces), which have an excess volume and/or reduce the local coordination number.

The sulfur–sulfur interaction is found to be repulsive at the first nearest neighbor distance in the f.c.c. copper matrix, whereas it is attractive at the second nearest neighbor distance. This is also consistent with the local coordination in copper sulfide where the S–S distance is larger than the Cu–Cu or Cu–S distances. The interactions of S with both the Ag and P impurities in the first coordination shell are repulsive, as well as the interactions for the P–P and the Ag–Ag defect pairs. However, the interactions of these impurities with vacancies are attractive, though they are not as strong as the S–Vac interaction.

Table 3. Pair interaction energies of point defects in f.c.c. Cu at first ($E^{int}_{X-Y,1}$) and second ($E^{int}_{X-Y,2}$) nearest neighbor distance. The energies are in eV

Defect pair, X–Y	$E^{int}_{X-Y,1}$	$E^{int}_{X-Y,2}$
S–S	+0.11	−0.12
P–P	+0.26	−0.03
Ag–Ag	+0.21	+0.06
Vac–Vac	−0.06	+0.06
S–P	+0.25	−0.05
S–Ag	+0.18	−0.01
S–Vac	−0.46	−0.03
P–Vac	−0.28	−0.04
Ag–Vac	−0.21	−0.00

We remark, that the accuracy of our calculations of the defect interaction energies (Table 3) is limited by the approximations used in the method (ASA + M and LDA) as well as by the residual defect interactions at the 8th coordination shell in the $2 \times 2 \times 4$ supercells and, finally, because of the contribution to the defect interaction energy due to local lattice relaxation around the defects, which is neglected in this study. Our calculations for single defects using 32- and 108-site supercells show that the possible error due to residual defect interactions is about 0.01 eV and can be neglected. The contribution due to local relaxation is more difficult to estimate without performing the corresponding calculations which are problematic within the ASA. Qualitatively, one may conclude that the energy of local relaxation around isolated impurities and the energy of local relaxation around a defect pair must cancel each other to a large extent when one calculates the defect interaction energy, equation (8), so the final contribution to the defect interaction energy should only be a fraction of the local relaxation energy of isolated impurities. We therefore expect that our calculations performed on a rigid lattice give qualitatively correct results containing the essential physical information about the defect interactions.

It also follows that some of the calculated defect interaction energies at second nearest neighbor distance are statistically insignificant and must be considered to be equal to zero because their values are within the accuracy of calculations. On the other hand, all the interactions in the first coordination shell are relatively strong and, therefore, reliable.

4. DISCUSSION

Let us first analyze the results of our calculations for the Cu–S binary system. Although the defect interactions have only a small effect on the equilibrium defect concentrations in the bulk, they must be of importance for the kinetics of the supersaturated solid solution decomposition as well as for the grain boundary segregation. Due to their strong attraction, the excess vacancies and sulfur impurities will form bound complexes on their way to the segregation sites. Once formed, such a complex will have a very low probability to dissociate and a high mobility in the crystal. Thus, each sulfur atom segregating to a grain boundary or to a dislocation brings at least one vacancy with it, thereby increasing the vacancy concentration in the vicinity of the defect. To understand the structure which the segregated sulfur atoms form, one therefore has to take into account the equivalent amount of co-segregating vacancies. It seems highly improbable that a S–Vac pair will dissociate after it has segregated to a defect. Rather, segregated sulfur–vacancy pairs will diffuse along the defect until they meet each other and form more extended defect arrangements.

In general, a knowledge of the pair defect interactions at first and second nearest neighbor distance in a dilute solid solution presented in Section 3.2 is not sufficient to determine the structure of a concentrated defect arrangement [20]. For this purpose one also needs pair defect interactions at longer distances as well as three- and four-body defect interactions. The volume dependence of the effective interatomic interactions may also be important. However, the S–S and S–Vac pair interactions at first and second nearest neighbor distance are the strongest interactions and they imply that in the concentrated defect arrangement sulfur atoms will tend to surround themselves with vacancies and avoid other sulfur atoms in the first coordination shell. One possible concentrated defect arrangement in f.c.c. Cu having the composition Cu_2S is shown in Fig. 1(b). The structure consists of alternating (001) S–Vac and Cu planes. The total energy calculations performed for this structure show that its formation energy (–0.14 eV/atom) is much lower than the calculated mixing energy of the corresponding random alloys having the same composition† either with (+0.25 eV/atom) or without vacancies (+0.07 eV/atom), but still it is well above the formation energy of copper sulfide Cu_2S. However, our calculations show that by changing the c/a ratio as shown in Fig. 1, this structure may be continuously transformed into the antifluorite structure of high digenite without an activation barrier.

Thus, our analysis shows that concentrated sulfur–vacancy defect arrangements have a strong ordering tendency towards a formation of copper sulfide. The knowledge of the defect interactions gives us a possible scenario of the supersaturated Cu–S solid solution decomposition. Very stable and mobile sulfur–vacancy complexes segregate to linear or planar defects in Cu, where they have a high probability to meet each other to form Cu_2S. The process of copper sulfide precipitation must have a low activation energy because it is favored by the defect interactions and it must occur at a high rate because of the high mobility of the S–Vac defect pairs.

Note, that from the technological point of view the precipitation of copper sulfide at grain boundaries is highly undesirable because depending on its composition this compound undergoes several structural transformations in the temperature interval of interest. These structural transformations as well as the mechanical properties of the copper sulfide should favor crack nucleation and propagation at grain boundaries under creep conditions.

†Concentrated random Cu–S alloys having the composition Cu_2S (with and without vacancies) were modeled in this work using $3 \times 3 \times 3$ (108 sites) f.c.c. supercells. The procedure of special quasirandom structure construction is described in Ref. [32].

Let us now analyze the effect of P or Ag additions to copper in terms of the defect interactions. Because of the repulsive S–P and S–Ag interactions, these impurities cannot increase the *equilibrium* solubility of sulfur in copper. Like sulfur, phosphorus and silver impurities have attractive interactions with vacancies. As these impurities have much larger solubility in the bulk copper than sulfur has, they will form impurity–vacancy pairs with a much higher probability, thus significantly decreasing the number of vacancies available for the sulfur atoms. The same kind of competition for the segregation sites is expected to take place at dislocations and grain boundaries. Therefore, the additions of P or Ag to Cu may considerably slow down the process of Cu_2S precipitation. As a result, the *non-equilibrium* solubility of sulfur in copper may increase, something which is actually observed in experiments [5].

Another important consequence of the competition for the lattice defects could be a blocking effect. The segregated phosphorus or silver will isolate the grain boundary areas enriched in sulfur from each other thus probably preventing the formation of large-scale Cu_2S precipitates. As the sulfide particles are the most probable centers of crack nucleation, the ductility of copper will increase upon a lowering of the size of Cu_2S inclusions.

5. CONCLUSIONS

In summary, the problem of medium temperature embrittlement of commercially pure copper is studied theoretically using electronic structure and total energy calculations within a supercell approach to model dilute copper alloys. The solution energies, volume misfits, and defect interaction energies for selected technologically important point defects in Cu are calculated. It is shown that the solubility of S in Cu is limited mainly because of the formation of a very stable intermediate phase, Cu_2S.

A strong attraction is found between a sulfur impurity and a vacancy in copper which leads to the formation of highly stable and mobile sulfur–vacancy defect complexes. The S–Vac and S–S pair interactions favor precipitation of copper sulfide at lattice defects like dislocations, grain boundaries and open surfaces where the local coordination number is reduced.

The analysis of the defect interactions shows that the main effect of phosphorus or silver additions to copper may consist in their competition to attract vacancies and other lattice defects. This results in a retardation of the kinetics of the supersaturated Cu–S solid solution decomposition combined with a refining of the size of the Cu_2S precipitates. As a consequence, the mechanical behavior of copper under creep conditions may improve upon phosphorus or silver additions.

Acknowledgements—This work is entirely funded by SKB AB, the Swedish Nuclear Fuel and Waste Management Company.

REFERENCES

1. Butron-Guillen, M. P., Cabanas-Moreno, J. G. and Weertman, J. R., *Scripta metall.*, 1990, **24**, 991.
2. Henderson, P. J., Österberg, J. O. and Ivarsson, B., Low temperature creep of copper intended for nuclear waste containers. SKB Technical Report TR 92-04, Swedish Nuclear Fuel and Waste Management Co., Stockholm, 1992.
3. Fujivara, S. and Abiko, K., *J. Physique IV (Colloque)*, 1995, **5**, 295.
4. Chakrabarti, D. J. and Laughlin, D. E., in *Binary Alloy Phase Diagrams*, 2nd edn, ed. T. B. Massalski. ASM International, 1990, p. 1467.
5. Smart, J. S. and Smith, A. A., *Trans. Am. Inst. Min. Engrs*, 1946, **166**, 144.
6. Oudar, J., *C. R. Acad. Sci.*, 1959, **249**, 259.
7. Van-Dyck, D., Conde-Amiano, C. and Amelinckx, S., *Physica status solidi*, 1980, **A58**, 451.
8. Gray, J. N. and Clarke, R., *Phys. Rev.*, 1986, **B33**, 2056.
9. Kashida, S. and Yamamoto, K., *J. Phys.: Condens. Matter*, 1991, **3**, 6559.
10. Berger, R. and Bucur, R. V., *Solid St. Ionics*, 1996, **89**, 269.
11. Madelung, O. (ed.), *Diffusion in Solid Metals and Alloys*, Landolt-Börnstein, New Series, Group III/26. Springer-Verlag, Berlin, 1990.
12. Surholt, T. and Herzig, Chr., *Acta mater.*, 1997, **45**, 3817.
13. Ehrhart, P., Jung, P., Schultz, H. and Ullmaier, H., in *Atomic Defects in Metals*, Landolt-Börnstein, New Series, Group III/25, ed. H. Ullmaier. Springer-Verlag, Berlin, 1991.
14. Braspenning, P. J., Zeller, R., Dederichs, P. H. and Lodder, A., *J. Phys. F: Metal Phys.*, 1982, **12**, 105.
15. Mertig, I., Mrosan, E. and Ziesche, P., *Multiple Scattering Theory of Point Defects in Metals: Electronic Properties*. Teubner Verlagsgeselshaft, Leipzig, 1987.
16. Abrikosov, I. A., Vekilov, Yu. Kh. and Ruban, A. V., *Russ. J. Inorg. Chem.*, 1990, **35**, 1046.
17. Abrikosov, I. A., Vekilov, Yu. Kh., Ruban, A. V. and Simak, S. I., *Soviet Phys. Dokl.*, 1990, **35**, 961.
18. Drittler, B., Weinert, M., Zeller, R. and Dederichs, P. H., *Phys. Rev.*, 1989, **B39**, 930.
19. Stefanou, N., Papanikolaou, N. and Dederichs, P. H., *J. Phys.: Condens. Matter*, 1991, **3**, 8793.
20. Klemradt, U., Drittler, B., Hoshino, T., Zeller, R., Dederichs, P. H. and Stefanou, N., *Phys. Rev.*, 1991, **B43**, 9487.
21. Hoshino, T., Schweika, W., Zeller, R. and Dederichs, P. H., *Phys. Rev.*, 1993, **B47**, 5106.
22. Hoshino, T., Zeller, R., Dederichs, P. H. and Asada, T., *Physica B*, 1997, **237-238**, 361.
23. Dederichs, P. H., Drittler, B. and Zeller, R., *Mater. Res. Soc. Symp. Proc.*, 1992, **253**, 185.
24. Papanikolaou, N., Zeller, R. and Dederichs, P. H., *Phys. Rev.*, 1997, **B55**, 4157.
25. Raybaud, P., Kresse, G., Hafner, J. and Toulhoat, H., *J. Phys.: Condens. Matter*, 1997, **9**, 11085.
26. Raybaud, P., Hafner, J., Kresse, G. and Toulhoat, H., *J. Phys.: Condens. Matter*, 1997, **9**, 11107.
27. Burdett, J. K. and Eisenstein, O., *Inorg. Chem.*, 1992, **31**, 1758.
28. Bratland, D. H., Grong, O., Shercliff, H., Myhr, O. H. and Tjotta, S., *Acta mater.*, 1997, **45**, 1.

29. Nicholson, D. M. C., Stocks, G. M., Wang, Y., Shelton, W. A., Szotek, Z. and Temmerman, W. M., *Phys. Rev.*, 1994, **B50**, 14686.
30. Wang, Y., Stocks, G. M., Shelton, W. A., Nicholson, D. M. C., Szotek, Z. and Temmerman, W. M., *Phys. Rev. Lett.*, 1995, **75**, 2867.
31. Abrikosov, I. A., Niklasson, A. M. N., Simak, S. I., Johansson, B., Ruban, A. V. and Skriver, H. L., *Phys. Rev. Lett.*, 1996, **76**, 4203.
32. Abrikosov, I. A., Simak, S. I., Johansson, B., Ruban, A. V. and Skriver, H. L., *Phys. Rev.*, 1997, **B56**, 9319.
33. Andersen, O. K., *Phys. Rev.*, 1975, **B12**, 3060.
34. Gunnarsson, O., Jepsen, O. and Andersen, O. K., *Phys. Rev.*, 1983, **B27**, 7144.
35. Skriver, H. L., *The LMTO Method.* Springer-Verlag, Berlin, 1984.
36. Andersen, O. K. and Jepsen, O., *Phys. Rev. Lett.*, 1984, **53**, 2571.
37. Andersen, O. K., Jepsen, O. and Glötzel, D., in *Highlights of Condensed-Matter Theory*, ed. F. Bassani, F. Fumi and M. P. Tosi. North-Holland, New York, 1985.
38. Andersen, O. K., Pawlowska, Z. and Jepsen, O., *Phys. Rev.*, 1986, **B34**, 5253.
39. Skriver, H. L. and Rosengaard, N. M., *Phys. Rev.*, 1992, **B46**, 7157.
40. Korzhavyi, P. A., Abrikosov, I. A., Johansson, B., Ruban, A. V. and Skriver, H. L., *Phys. Rev.*, 1999, **B59**, in press.
41. Perdew, J. and Zunger, A., *Phys. Rev.*, 1981, **B23**, 5048.
42. Ceperley, D. M. and Alder, B. J., *Phys. Rev. Lett.*, 1980, **45**, 566.
43. Drittler, B., Weinert, M., Zeller, R. and Dederichs, P. H., *Solid St. Commun.*, 1991, **79**, 31.
44. Hultgren, R., Orr, R. L., Anderson, P. D. and Kelley, K. K., *Selected Values of Thermodynamic Properties of Metals and Alloys.* John Wiley, New York, 1963.
45. Pearson, W. B., *A Handbook of Lattice Spacings and Structures of Metals and Alloys.* Pergamon Press, London, 1958.
46. Barin, I. and Knacke, O., *Thermochemical Properties of Inorganic Substances.* Springer-Verlag, Berlin, 1973.